FOURTH U.S.-N.Z.-Japan-China Seminar on Design of Reinforced Concrete Beam-Column Joints, Hawaii, May 24-26, 1989.

COMPARISON OF TEST RESULTS ON QUADRI-LATERAL PROGRAMME

by

Kazuhiro KITAYAMA

Department of Architecture
Faculty of Engineering
Utsunomiya University
Utsunomiya-city, Tochigi 321

INTRODUCTION

The tests of three-dimensional beam-column joints with slabs were executed as the quadri-lateral cooperative research project in the United States, New Zealand, Japan and China. The main objective of the programme is to investigate the behavior of reinforced concrete beam-column-slab subassemblages designed in accordance with the building code or the standards of the respective countries.

In this paper, the test results of the programme are compared briefly focusing on the hysteretic behavior, joint shear under the uni-directional and bi-directional loading, and the bond condition along the beam reinforcement passing through an interior joint.

SPECIMENS

Seventeen specimens, among which nine specimens are interior beam-column joints and eight exterior beam-column joints, were tested on quadri-lateral programme. Two specimens tested in Kyoto University by Fujii and Morita are included in this paper because these specimens were loaded according to the guidelines decided at the Second U.S.-N.Z.-Japan Seminar, Tokyo, 1985 (Ref.1). The general properties of the specimens are summarized in Table.1. All specimens except specimens in Japan were full scale models, whereas five specimens in Japan were half or one-third scale models depending on the loading apparatus. All specimens were designed to develop a beam flexural yielding prior to a column yielding or joint shear failure in accordance with the seismic provisions in respective countries.

The lateral reinforcement ratio in a joint was approximately 0.3 %, 0.6 %, 0.9 % and 1.2 % for specimens in Japan, the United States, China and New Zealand, respectively. The difference of the amount of the joint lateral reinforcement seems to be attributed to the assumed shear resisting mechanism of a joint and the construction method in each countries. Joint lateral reinforcement ratio is defined as the total cross-sectional area of the lateral reinforcement between the beam top and bottom bars divided by the column width and the distance of (7/8)d, d: beam effective depth.

CALCULATION OF RESISTANCES

The ratios of a column to beam moment capacity are summarized in

Table.2. These ratios are very conservative since the flexural strength of a column was defined as the moment corresponding to the yielding of the longitudinal reinforcement in the most outer layer, and that of a beam was calculated assuming the entire slab width effective to the beam resistance except specimens in the United States. The strength ratio of a column to beam under the bi-directional loading was calculated on the assumption that the bi-directional interaction capacity surface of a column forms a circle, whereas that of a beam is represented by the two orthogonal lines. The ratios under the uni-directional loading were greater than 1.2, and those under the bi-directional loading greater than 1.0 in most of specimens, indicating that a column yielding does not occur even in the bi-directional loading.

TEST RESULTS

Failure Mode and Joint Shear: All specimens developed a beam flexural yielding and maintained the beam collapse mechanism during the test without a remarkable strength decay. However, several specimens were pointed out by researchers to fail in joint shear at a story drift angle more than 1/25 rad after the beam yielding. The hysteretic behavior of all specimens was considered to be satisfactory up to a story drift angle of 1/50 rad.

The maximum joint shear stresses under the uni-directional loading are summarized in Table.3 and plotted in Fig.1 with the lateral reinforcement ratio in a joint. The effective joint area to resist shear is defined by the column depth in an interior joint, or the horizontally projected length in an exterior joint and the average of the beam and column widths. Joint shear stresses normalized by the concrete compressive strength v_p/fc' were distributed from 0.12 fc' to 0.47 fc' for interior joints, and from 0.09 fc' to 0.29 fc' for exterior joints. The normalized joint shear stresses of specimens in New Zealand and China were smaller than those in Japan and the United States. The joint shear failure after beam flexural yielding occurred when the maximum shear stress was greater than 0.35 fc' in interior joints, and 0.2 fc' in exterior joints. The maximum joint shear observed in the United States specimens exceeded the design shear of $15\sqrt{fc'}$ or $20\sqrt{fc'}$ (fc' in psi) recommended by ACI-ASCE 352 Committee (Ref.8).

The joint shear resultant under the bi-directional loading is summarized in Table.4 and shown in Fig.2. The effective joint area to resist shear is defined by the gross sectional area of a column. Open symbols represent the interior joint specimens. The shear under the bi-directional loading was less than the square root of sum of the squares of maximum shear forces in respective directions. This was caused by the degradation of resistance in one direction due to the bi-axial interaction of resistances. Note that the joint shear stress normalized by the concrete compressive strength under the bi-directional loading $v_{p,b}/fc'$ is not always larger than that under the uni-directional loading because the effective joint area to resist shear is different in two loading cases.

The joint shear in respective directions at the maximum resultant under the bi-directional loading is shown in Fig.3. Solid lines represent the bi-axial interaction of shear resistances in an interior joint assumed to be a circle or two orthogonal lines, and broken lines represent that in an exterior joint. The joint shear strength in one direction was assumed to be 0.30 fc' in interior joints and 0.18 fc' in exterior joints according to the provisions in Japan (Ref.9). Maximum shear in the interior joint of Specimen J2A, resulted in joint shear failure after the beam flexural yielding, exceeded the joint shear strength assumed to form a square

without the bi-axial interaction. On the contrary, exterior joints of Specimens J3A, GBS3 and GBSU failed in joint shear after the beam flexural yielding, reaching the shear strength assumed to form an ellipse. Note that the joint shear strength of 0.30 fc' in an interior joint is fairly conservative, whereas that of 0.18 fc' in an exterior joint should be reduced taking the bi-axial interaction of joint shear resistances into account. Beams framing into four faces of a joint and slabs may contribute to enhance the shear strength of an interior joint.

Stifness in Story Shear-Drift Relation: Secant modulus in story shear-drift relations at story drift angles of 1/200 rad and 1/100 rad were calculated and shown in Fig.4. Large secant moduli were observed in Specimens 2D-I, K2 and 1D-I, developing the yielding of beam bars by a story drift angle of 1/100 rad approximately. On the other hand, the secant modulus of specimens in the United States, in which beam reinforcing bars started to yield at a story drift angle greater than 1/80 rad, were less than the half of those in Specimens 2D-I and K2.

Story Drift at Maximum Joint Shear: Joint shear in most specimens increased gradually after beam flexural yielding to the end of the test, i.e., to the story drift angle greater than 1/25 rad. Specimens 2D-I and 2D-E in New Zealand reached the maximum joint shear at the story drift angle of 1/53 rad and 1/100 rad, respectively, developing the yielding of the slab reinforcement within an entire slab width.

Energy Dissipation and Beam Bar Bond: To estimate the energy dissipating ability, the equivalent viscous damping ratio h_{eq}, ratio of the dissipated energy within half a cycle to 2 π times the strain energy at the peak of an equivalent linearly elastic system, is used.

The possibility of bond degradation along the beam reinforcement passing through an interior joint is indicated by "beam bar bond index $u_b/\sqrt{fc'}$" (Ref.10), where u_b is the average bond stress over the column width for simultaneous yielding of the beam reinforcement in tension and compression at the two faces of a joint as expressed below, and fc' is the concrete compressive strength in kgf/cm^2.

$$u_b = f_y (d_b / h_c) / 2 \qquad (1)$$

where f_y: yield strength of beam bars in kgf/cm^2, d_b: diameter of beam bars, and h_c: column width.

The beam bar bond index $u_b/\sqrt{fc'}$ and the equivalent viscous damping ratio h_{eq} at a story drift angle of 1/50 approximately are compared in Fig.5 and summarized in Table.5 for interior joint specimens. When the beam bar bond index was different between the beam top and bottom reinforcement, whichever is larger was chosen in Fig.5. The solid line was derived from the least squares method to fit the data for the plane beam-column joints tested previously in Japan (Ref.10). The equivalent viscous damping ratio h_{eq} decreased with an increasing $u_b/\sqrt{fc'}$ value, indicating that the bond along the beam reinforcement deteriorated. Values of $u_b/\sqrt{fc'}$ and h_{eq} were largely different between specimens in New Zealand and the United States. This was caused by the difference of the required performance of reinforced concrete buildings under earthquake motions. In New Zealand, the beam reinforcing bars with a small diameter and low strength are used, maintaining a good bond within a joint.

Note that the h_{eq} values except Specimens J1C and J2C without slabs

were smaller than that of the value obtained from the least squares method in the test results of plane beam-column joints. This might be caused by the delay in crack closing attributable to shift in the location of the neutral axis above the beam top reinforcement under positive bending (the beam top fiber in compression) in Specimen K2 (Ref.2), or by the shear distress in a joint and the flexural distress in a slab, beam and column in Specimens J1A and J2A (Ref.3).

Stress Distribution of Slab Bars: The stresses in the slab reinforcement parallel to the longitudinal beam increased with the story drift under negative bending, and reached the yield stress in most of the slab bars at a story drift angle of 1/50 rad in Japanese and New Zealand specimens as shown in Fig.6. The effective slab width of specimens in the United States was determined to be 60 % of the entire slab width at a story drift angle of 1/25 rad.

CONCLUDING REMARKS

The hysteretic behavior of test specimens on quadri-lateral programme was considered to be satisfactory under the bi-directional cyclic load reversals up to a story drift angle of 1/50 rad, although the joint shear stress normalized by concrete compressive strength and the bond performance along the beam reinforcement differed distinctly among specimens of four countries. Joint shear failure was developed at a story drift angle of 1/25 rad after the beam yielding by the high joint shear larger than 0.4 fc' in three-dimensional interior joints and 0.2 fc' in exterior joints.

The influence of the pinching in a hysteresis loop resulted from the bond deterioration along the beam bars and the joint shear distortion should be investigated on earthquake responses of reinforced concrete structures.

REFERENCES

1. Minutes of the Second U.S.-N.Z.-Japan Seminar on Design of Reinforced Concrete Beam-Column Joints, May 28 and 29, 1985, in Tokyo, Aoyama Laboratory, University of Tokyo.

2. Kitayama, K., S. Otani and H. Aoyama, : Behavior of Reinforced Concrete Beam-Column-Slab Subassemblages Subjected to Bi-Directional Load Reversals, Proceedings of Ninth World Conference on Earthquake Engineering , Vol.VIII, August, 1988, pp.VIII 581-586.

3. Kurose, Y., G. N. Guimaraes, Z. Liu, M. E. Kreger and J. O. Jirsa, : Study of Reinforced Concrete Beam-Column Joints under Uniaxial and Biaxial Loading, the University of Texas at Austin, PMFSEL Report, No.88-2, December, 1988.

4. Cheung, P. C., T. Paulay and R. Park, : Interior and Exterior Reinforced Concrete Beam-Column Joints of a Prototype Two-Frame with Floor Slab Designed for Earthquake Resistance, University of Canterbury, Research Report, 89-2, March, 1989.

5. Chen, Y., G. Chen and H. Gao, : Full Scale Tests on Seismic Behavior of Internal Reinforced Concrete Beam-Column Joints under Bidirectional Cyclic Loading, paper prepared for the Third U.S.-N.Z.-Japan-China Seminar on the Design of Reinforced Concrete Beam-Column Joints, August 10 to 12, 1987, at University of Canterbury, Christchurch.

6. Zhu, B., and Y. Chen, : Behavior of Exterior Reinforced Concrete Beam-Column Joints Subjected to Bi-Directional Cyclic Loading, paper prepared for the Third U.S.-N.Z.-Japan-China Seminar on the Design of Reinforced Concrete Beam-Column Joints, August 10 to 12, 1987, at University of Canterbury, Christchurch.

7. Fujii, S., and S. Morita, : Behavior of Exterior Reinforced Concrete Beam-Column-Slab Subassemblages under Bi-Directional Loading, paper prepared for the Third U.S.-N.Z.-Japan-China Seminar on the Design of Reinforced Concrete Beam-Column Joints, August 10 to 12, 1987, at University of Canterbury, Christchurch.

8. ACI-ASCE Committee 352, : Recommendations for Design of Beam-Column Joints in Monolithic Reinforced Concrete Structures, ACI-ASCE 352 R-85, ACI Journal, Vol.82, No.3, May-June 1985, pp.266-283.

9. Architectural Institute of Japan, : Design Guideline for Earthquake Resistant Reinforced Concrete Buildings Based on Ultimate Strength Concept (in Japanese), 1988.

10. Aoyama, H., S. Otani and K. Kitayama, : Design Criteria for Reinforced Concrete Interior Beam-Column Connections, Proceedings of Ninth World Conference on Earthquake Engineering, Vol.IV, August, 1988, pp.IV 615-620.

Table 1 : Specimens Tested in Quadri-lateral Programme

Specimen (Label in this paper)	Type	Column Section bxD mm	Beam Section bxD mm	Slab Thick-ness mm	Height mm	Length mm	Concrete Compressive Strength kgf/cm^2	Researcher (Ref.No.)
K1	Interior Two-way	275x275	L: 200x300 T: 200x285	70	1470	2700	244 U.C. 266	
K2	Interior Two-way	375x375	L: 200x300 T: 200x285	70	1470	2700	244 U.C. 266	Kitayama Otani Aoyama
K3	Exterior Two-way	275x275	L: 200x300 T: 200x285	70	1470	L: 1350 T: 2700	199 U.C.196	(2)
J1 (J1A)	Interior One-way	508x508	406x508	127	4191	4877	246 U.C.247	
J2 (J2A)	Interior Two-way	508x508	L: 406x508 T: 406x508	127	4191	4877	282 U.C.266	Kurose Guimaraes Liu
J3 (J3A)	Exterior Two-way	508x508	L: 406x508 T: 406x508	127	4191	L: 2439 T: 4877	330 U.C.228	Kreger Jirsa (3)
1D-I	Interior One-way	550x600	400x550	100	3500	4055	388 U.C.269	
2D-I	Interior Two-way	600x600	L: 400x575 T: 400x550	100	3500	L: 4052 T: 4064	377 U.C.279	Cheung Paulay Park
2D-E	Exterior Two-way	500x550	L: 400x550 T: 300x575	100	3500	L: 2025 T: 4052	487 U.C.435	(4)
J1 (J1C)	Interior Two-way	600x600	L: 350x550 T: 350x550	none	3000	4000	492	
J2 (J2C)	(Same as Specimen J1C)							Chen Chen Gao
J3 (J3C)	Interior Two-way	600x600	L: 350x550 T: 350x550	130	3000	4000	476	(5)
J4	Exterior Two-way	600x600	L: 350x550 T: 350x550	none	3000	L: 2000 T: 4000	429	
J5	(Same as Specimen J4)							Zhu Chen
J6	Exterior Two-way	600x600	L: 350x550 T: 350x550	130	3000	L: 2000 T: 4000	373	(6)
GBS3	Exterior Two-way	220x220	L: 175x250 T: 160x250	60	1500	L: 1000 T: 1950	391	Fujii Morita
GBSU	(Same as Specimen GBS3 except fc', lateral reinforcement ratio in a joint, and beam bottom bars bent upwards)						354	(7)

Note: b : column or beam width, D : column or beam depth
L : longitudinal direction, T : transverse direction
U.C. : upper column

Table 2 : Ratio of Column to Beam Theoretical Moment Capacities

Specimen	Ratio under uni-directional loading *1		Ratio under bi-directional loading *2
	Longi. Dir.	Trans. Dir.	
K1	1.51	1.59	1.09
K2	1.81	1.92	1.32
K3	2.27	1.88	1.45
J1A	1.07	-	-
J2A	1.42	1.44	1.01
J3A	1.62	1.42	1.07
1D-I	1.65	-	-
2D-I	1.62	1.70	1.17
2D-E	2.50	1.86	1.46
J1C	1.93	1.92	1.36
J2C	(Same as Specimen J1C)		
J3C	1.21	1.20	0.85
J4			
J5			
J6			
GBS3	1.34	1.37	0.96
GBSU	1.33	1.37	0.95

Note: *1 Entire slab width was assumed to participate in the beam resistance for all specimens except Specimens J1A, J2A and J3A, of which slab width of 0.6 B was assumed to be effective, where B is the entire slab width.

*2 Ratio of column flexural strength to square root of sum of the squares of beam flexural strengths in two directions

Table 3 : Maximum Joint Shear under Uni-directional Loading

(a) Interior Joints

Specimen	Joint Shear tonf	Joint Shear Stress, $_2v_p$ kgf/cm^2	fc' kgf/cm^2	v_p/fc'	Failure Mode
K1	59.5	91.1	244	0.37	B
K2	63.7	59.1	244	0.24	B
J1A	205.0	88.3	246	0.36	BJ
J2A	306.1	131.8	282	0.47	BJ
1D-I	162.2	56.9	388	0.15	B
2D-I	176.0	58.7	377	0.16	B
J1C	171.2	60.1	492	0.12	B
J2C	(unknown)				B
J3C	(unknown)				BJ

Note: The joint effective area to resist shear was defined by the column depth and the average of the beam and column widths.
fc': concrete compressive strength
B : beam flexural failure
BJ : joint shear failure after beam flexural yielding

(b) Exterior Joints

Specimen	Joint Shear tonf	Joint Shear Stress, $_2v_p$ kgf/cm^2	fc' kgf/cm^2	v_p/fc'	Failure Mode
K3	32.4	57.3	199	0.29	B
J3A	190.0	92.6	330	0.28	BJ
2D-E	95.3	41.5	487	0.09	B
J4	162.0	68.2	429	0.16	B
J5	(unknown)				B
J6	(unknown)				B
GBS3	33.5	86.1	391	0.22	BJ
GBSU	32.8	84.3	354	0.24	BJ

Note: The joint effective area to resist shear was defined by the horizontally projected length and the average of the beam and column widths.
fc': concrete compressive strength
B : beam flexural failure
BJ : joint shear failure after beam flexural yielding

Table 4 : Maximum Joint Shear under Bi-directional Loading

Specimen	Resultant Joint Shear tonf	Joint Shear Stress, v_{2p} kgf/cm^2	v_p/fc'
K1	66.8	88.3	0.36
K2	77.1	54.8	0.22
K3	48.7	64.4	0.32
J2A	311.2	120.6	0.43
J3A	223.9	86.8	0.26
2D-I	212.4	59.0	0.16
2D-E	135.7	49.3	0.10
J2C	194.9	54.1	0.11
J3C	265.4	73.7	0.15
J5	151.8	42.2	0.09
J6	208.4	57.9	0.16
GBS3	36.1	74.6	0.19
GBSU	37.3	77.1	0.22

Note: The joint effective area to resist shear under bi-directional loading was defined by the column gross section.

Table 5 : Equivalent Viscous Damping Ratio and Bond Index

Specimen	Equivalent Viscous Damping Ratio, h_{eq}	u_b Top	u_b Bot. kgf/cm^2	$u_b/\sqrt{fc'}$ Top	$u_b/\sqrt{fc'}$ Bot.
K1	0.07 (Longi. Dir.)	102.1		6.54	
K2	0.12 (Longi. Dir.)	56.7		3.63	
K3	0.10 (Trans. Dir.)	77.3		5.48	
J1A	0.05	118.1	100.8	7.53	6.43
J2A	0.04 (Longi. Dir.)	118.1	98.1	7.03	5.84
1D-I	0.19	57.7		2.93	
2D-I	0.15 (Longi. Dir.)	57.7		2.97	
J1C	0.19	93.3	74.2	4.21	3.35
J2C	0.20	93.3	74.2	4.21	3.35

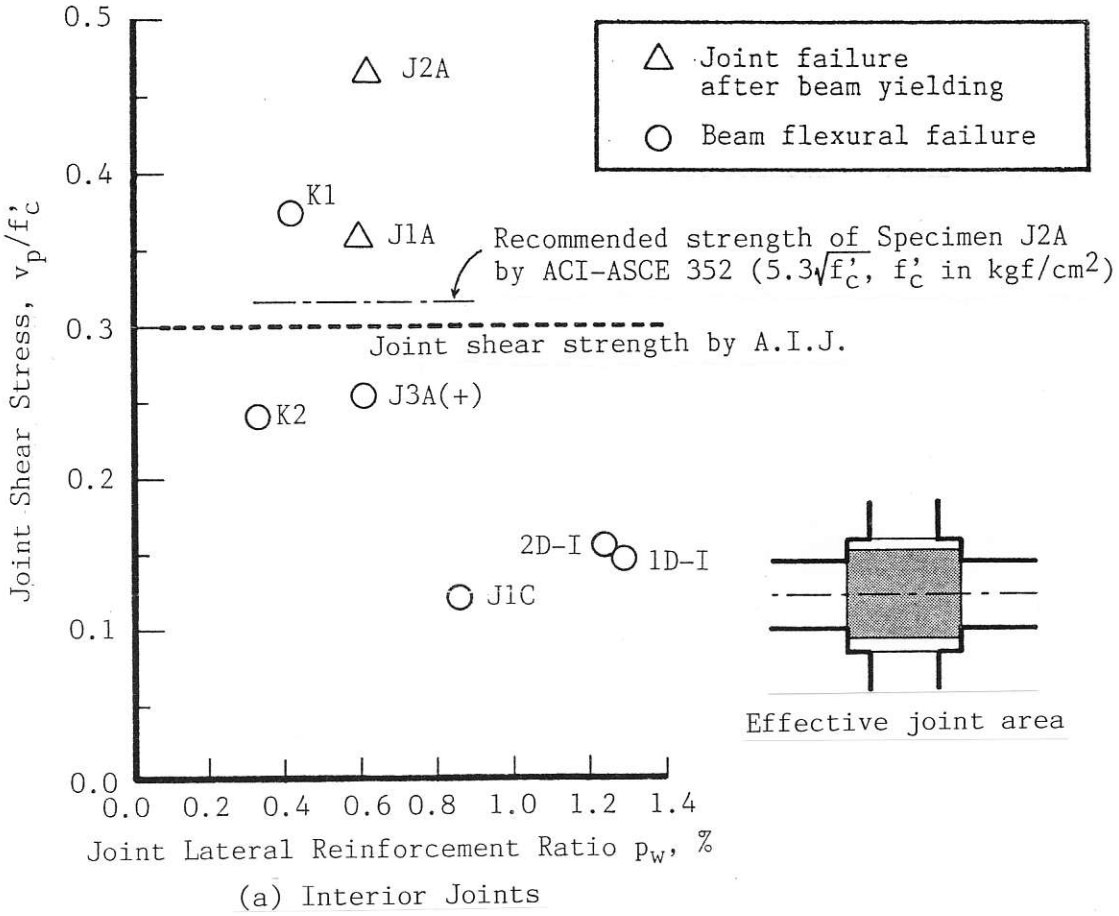

(a) Interior Joints

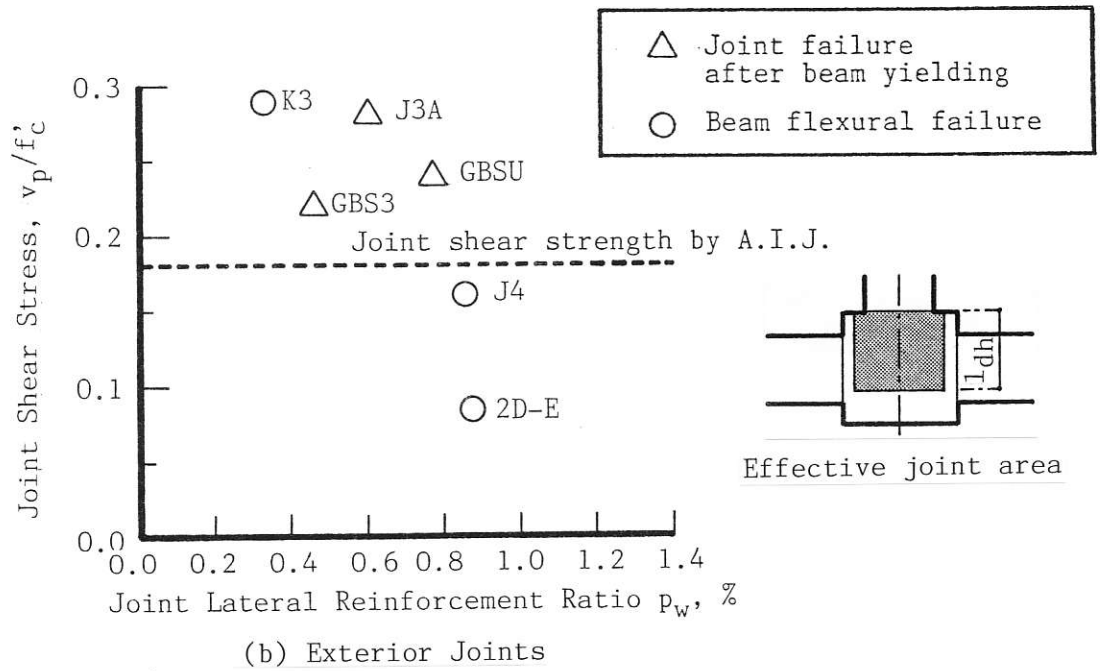

(b) Exterior Joints

Fig.1 : Joint Shear Stress under Uni-Directional Loading

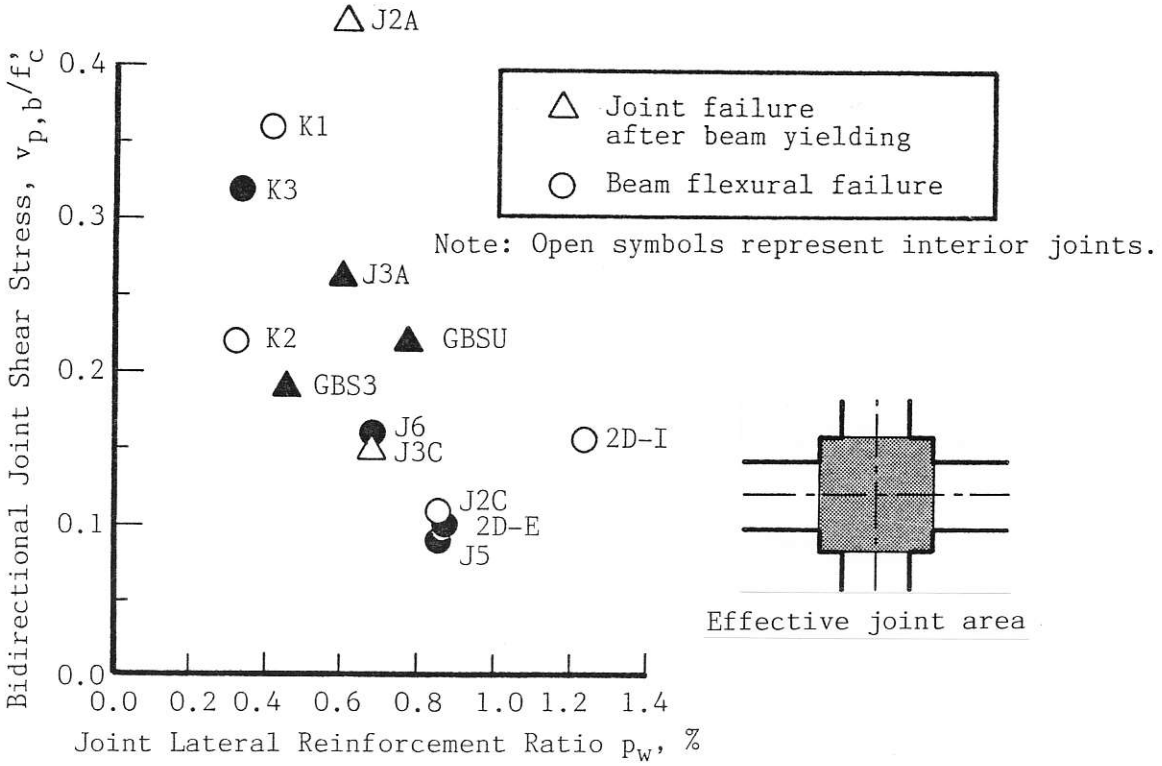

Fig.2 : Joint Shear Resultant under Bi-Directional Loading

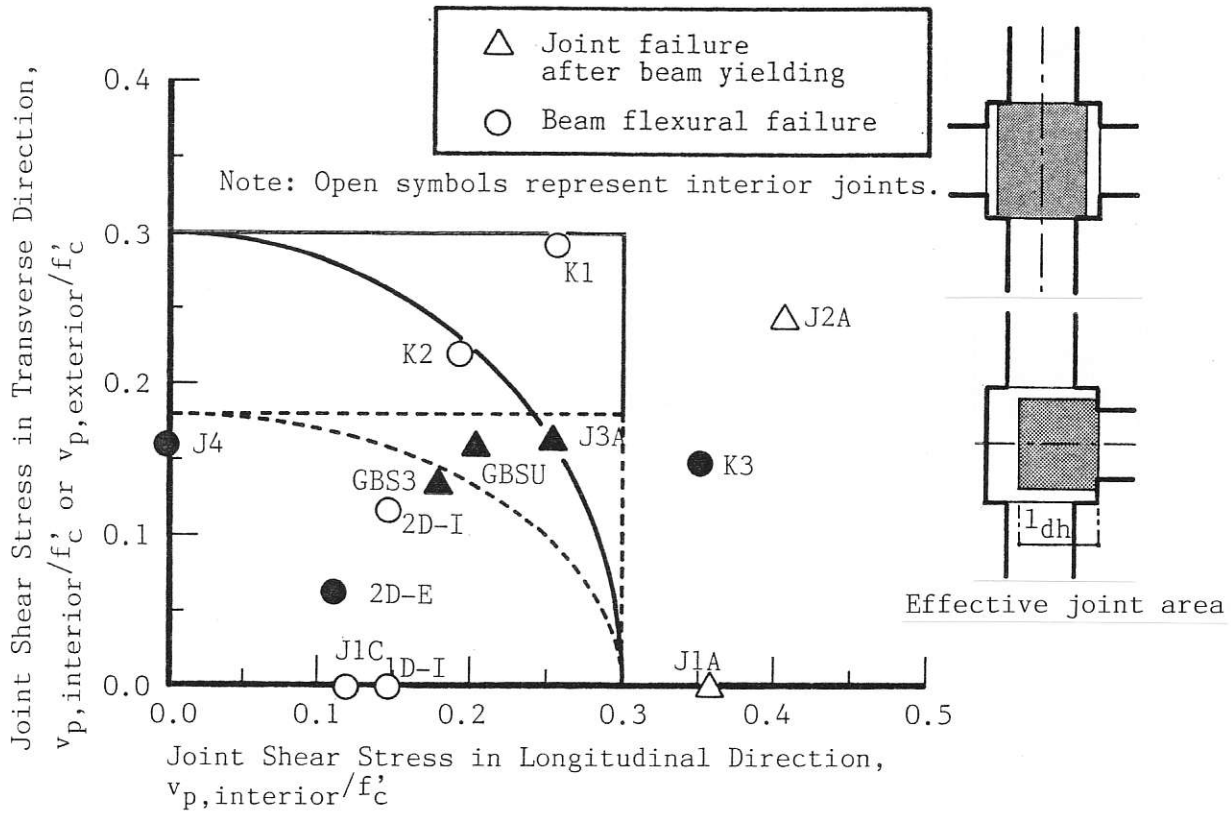

Fig.3 : Joint Shear Stresses under Bi-Directional Loading

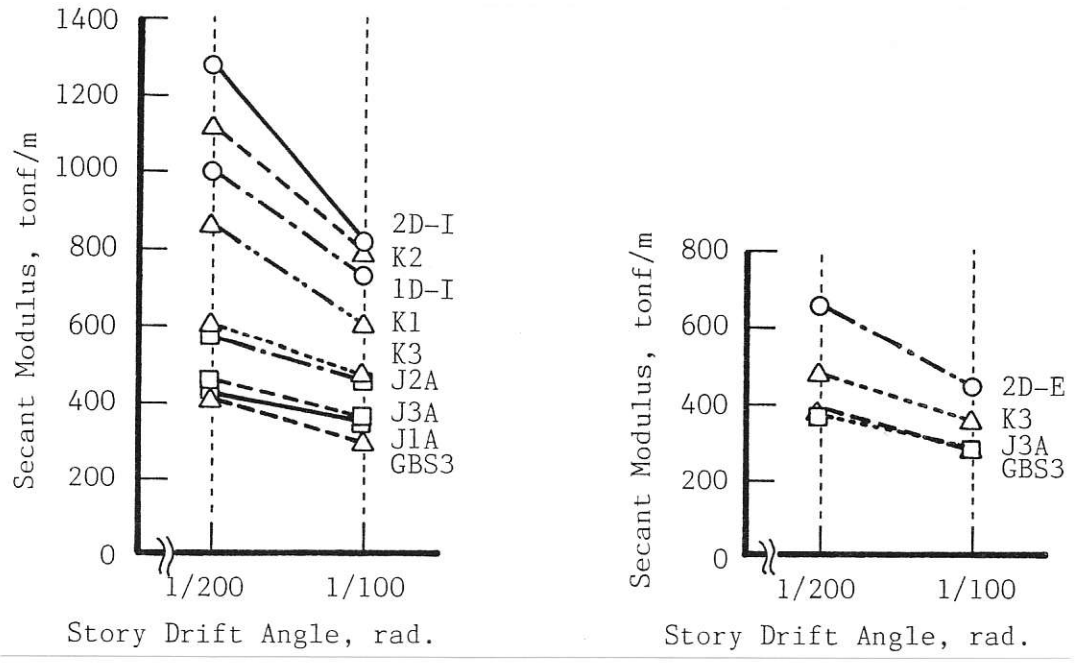

Fig.4 : Secant Modulus in Story Shear-Drift Relation

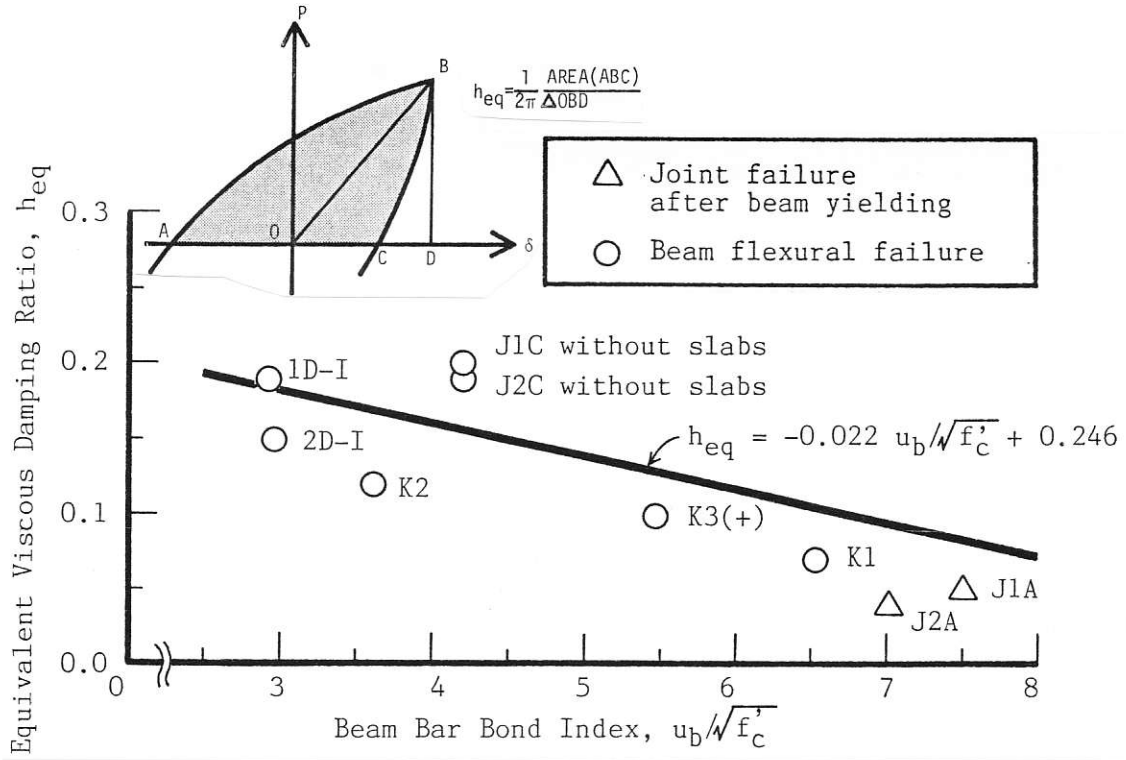

Fig.5 : Equivalent Viscous Damping Ratio - Beam Bar Bond Index Relation

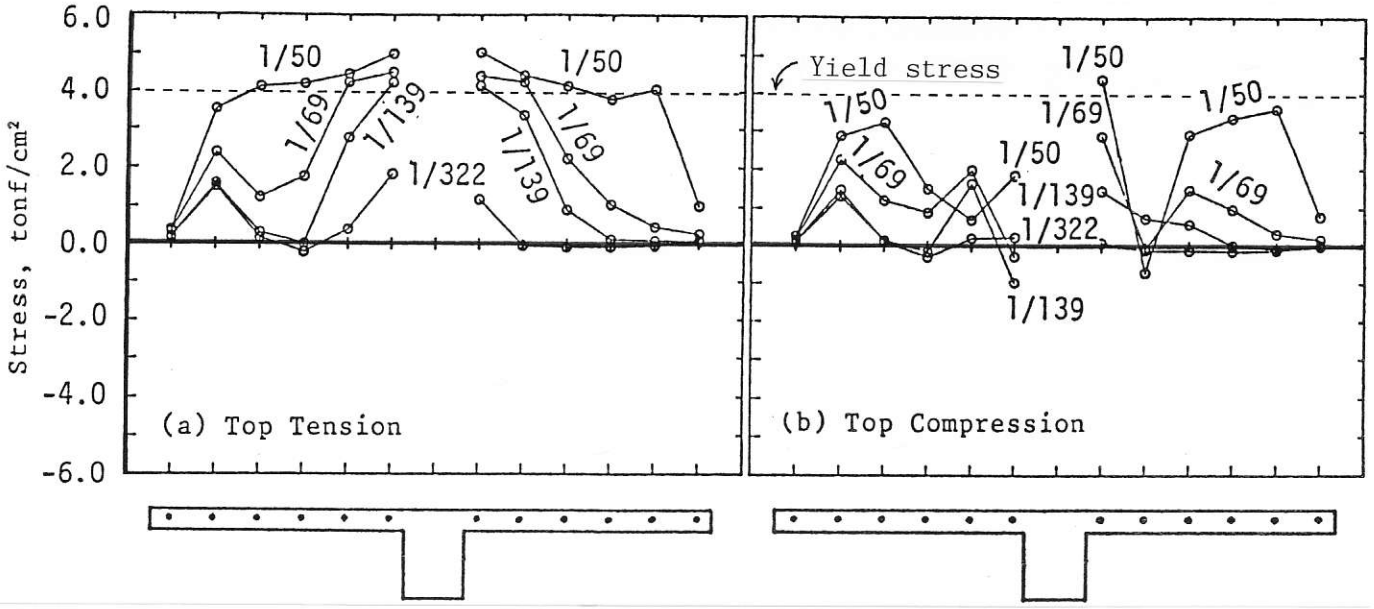

(a) Specimen K1 in Japan

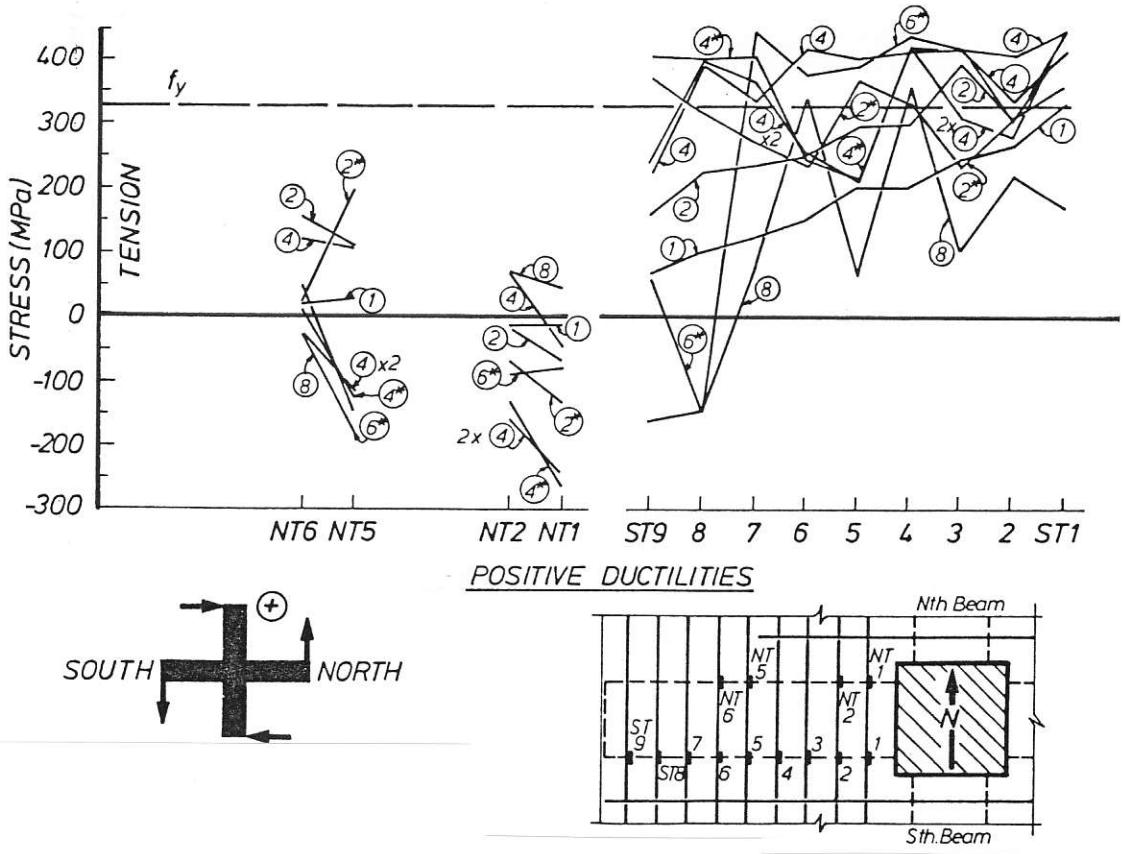

(b) Specimen 2D-I in New Zealand

Fig.6 : Stress Distributions of Slab Reinforcement